Evaluation of Lumbar Spine Muscle Forces

MOHAMMAD HAGHPANAHI[1], MARZYIEH ESMAILI[2]

Department of mechanical engineering

Iran University of Science and Technology

Tehran, Iran

IRAN

Abstract: - This work aimed to evaluate lumbar spine muscle forces under optimal posture. For this purpose, a parametric nonlinear finite element model of the lumbar spine with ten parameters is used. L1- L5 data were obtained from computed tomography (CT) (at 1mm wide increment) of the lumbar spine of a 30- year-old man. The advantage of parametric model is that it can be used for everyone with changing the parameters. A sagittally symmetric muscle architecture with 46 local muscles are used. The concept of optimal posture is explored by minimizing the segmental sagittal moments required for the equilibrium of the passive lumbar spine under a total of 2800 N axial compression while varying the lumbar lordosis. For the optimal posture, muscle forces are evaluated by an iteration method between lumbar spine FEM and an optimization technique. Some flattening in the lumbar spine substantially reduces the required moments and internal passive shear forces. Small muscle forces are calculated for this optimal posture. Furthermore, sensitivity of muscle forces to parameters of optimization is considered and desired optimization method which resulting to activation of more muscles, is selected.

Key-words: Lumbar spine, Parametric finite element model, Muscle force, Optimal posture, Optimization.

1 Introduction

Precise determination of load division among muscles and other components of the lumbar spine such as ligaments, facet joints, discs and vertebras is important both to assess risk of injury and and effective prevention, evaluation and treatment of spinal disorders. Moreover, the spine is stabilized by muscle forces. Thus, the muscle forces are an important factor for the spinal loading. A direct quantitative measurement of muscle forces is not possible. EMG allows the estimation of muscle forces after loading the upper body with a given moment [1]. However, many nonrigid factors affect the EMG signal amplitude. Thus in most positions, including standing and flexion of the upper body, precise determination of muscle forces from an EMG is not possible. Wilke et al. (2003) performed an extensive in vitro study with human cadaver lumbar spines [20]. After applying the upper body weight in different flexion/extension positions, muscle forces were varied until the bending moment at the L1 vertebra was zero. Several loading combinations were studied and the intersegmental rotations, intradiscal pressures and loads on the internal fixators were measured. The results were compared with those of in vivo measurements. Mostly a good agreement could be achieved, except for flexion of the upper body where a significant difference in the fixator loads was ascertained. Due to the difficulty and invasiveness of direct measurements, an analytical model of the lumbar spine, such as a finite element model (FEM), can be a valuable tool in determining the muscle forces and internal loads of the lumbar spine. In 2006 Rohlmann et al. determined trunk muscle forces for flexion and extension by using a validated finite element model of the lumbar spine and measured in vivo data [2]. To overcome kinetic redundancy, various approaches based on the reduction method, the EMG-assisted model, the optimization method or a combination of these have been used [7]. Shirazi Adl et al. developed and examined a novel kinematics-based approach that accounts for the synergy in the passive-active sub-systems while exploiting a priori known kinematics [10,11].The aim of this study was to determine lumbar spine muscle forces under optimal

posture. We used kinematics-based algorithm used by Shirazi Adl et al. The important difference is that we used this approach for a parametric nonlinear finite element model. The advantage of this model is that it can be used for everyone only with changing the parameters. This means that one program can be written that its input is the geometrical data from CT scan or MRI and the output is muscle forces of lumbar spine.

2 Materials and methods

2.1 Finite element model

The current study uses parametric nonlinear finite element model of the entire L1-L5 ligamentous lumbar spine (Fig.1). Its geometry is parametric and can be defined by a set of geometric parameters (10 for each vertebra) which can be measured from CT scans. The commercially available finite element program, ANSYS was used to model the spinal segments. Computer assisted tomographic images of the normal ligamentous lumbar spine of a 30-year-old male subject were obtained using transverse slices at every 1-mm interval. The analysis of the images are carried out in mimics software. With mimics we can obtain geometrical data of rigid tissues such as vertebral bodies.

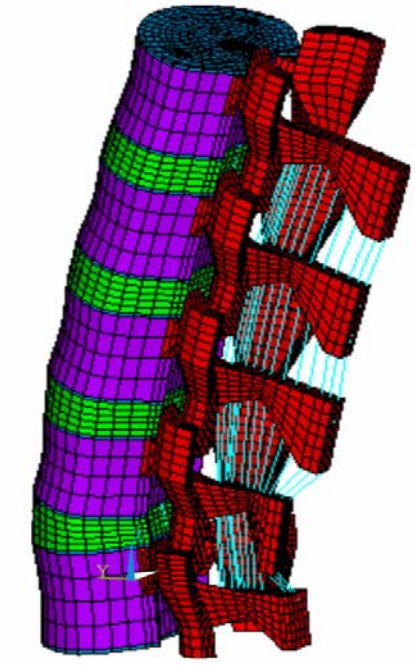

Fig.1. FEM of the entire lumbar spine (L_1-L_5)

The edge of the spinal disc was obtained from the enhanced CT images. But the geometry of the disc nucleus was difficult to distinguish from the CT image and the study referred to Panagiotacopulos et al.'s study [15]. The 30–50% of the total disc area in cross-section was defined as the disc nucleus of the FEM, and the rest of the region was assumed as the disc annulus of the FEM. The FEM of the ligamentous lumbar spine consisted of vertebrae, intervertebral discs, superior and inferior facet articulating surfaces, and a number of ligaments: supraspinous, interspinous, ligamentum flavum, transverse, posterior longitudinal, anterior longitudinal, and capsular. The material properties adopted from literature [4,5,6] are listed in Table 1. The nonlinear spring and cable elements were used to simulate ligaments and annulus fiber of disc, respectively.

The nonlinear properties of ligaments are shown in Fig 3 [8]. The facet joint was treated as a nonlinear three-dimensional contact problem using surface-to-surface contact elements, and the friction coefficient was set at 0.1 [9].

2.2 Boundary and loading condition

In the five-level FEM, the degrees of freedom of inferior surfaces of the L5 vertebral body were completely fixed in all directions. To validate the model, same loading conditions as given in Yamamoto et al.'s [18] and Chen-Sheng Chen et al.'s studies [19] were applied. Therefore, the 10 Nm flexion, 10 Nm extension and 10N m lateral bending moment under the 150 N pre-load were imposed on the L1 vertebral body, respectively.

2.3 Changes in posture and optimal sagittal posture

For the model, under up to 2800 N axial compression (80% applied at the L1 center and the rest distributed equally among the remaining vertebral centers to represent gravity loads, external loads and upper muscle forces [13]. initially all the L1-L5 vertebrae are constrained in sagittal/lateral rotations (i.e. no change in the posture) and the required equilibrating sagittal/lateral moments at all levels are evaluated. This is then followed by altering the posture in the sagittal plane by varying the lumbar lordosis while seeking a posture that reduces the foregoing moments at L1-L5 levels.

2.4 Muscle model and muscle force calculation

A sagittally symmetric muscle architecture with 46 local muscles (attached to the L1–L5 vertebrae) are used (Figs. 3 and 4): iliopsoas (IP), iliocostalis (IC), longissimus (LG), multifidus (MF) and quadrates lumborum (QL) as local muscles attaching the pelvis to lumbar vertebrae (except the IP that originates from the

Table 1 Element types and material properties used in the FEM. The material properties used were derived from the literature [4,5,6]

Component	Element type	Number of elements	E(Mpa)	Poisson ratio
Cortical Bone	8-Node solid	168	12000	0.3
Cancellous Bone	8-Node solid	1192	100	0.2
Boney posterior elements	8-Node solid	1280	3500	0.25
End plate	8-Node solid	352	25	0.3
Annulus matrix	8-Node solid	770	4.2	0.45
Annulus fibrosus	3-D Cable	448	175	-
Nucleus	8-Node solid	830	1	0.499
Facet joints	3-D Contact	560	-	-
Ligaments	Nonlinear spring	45	-	-

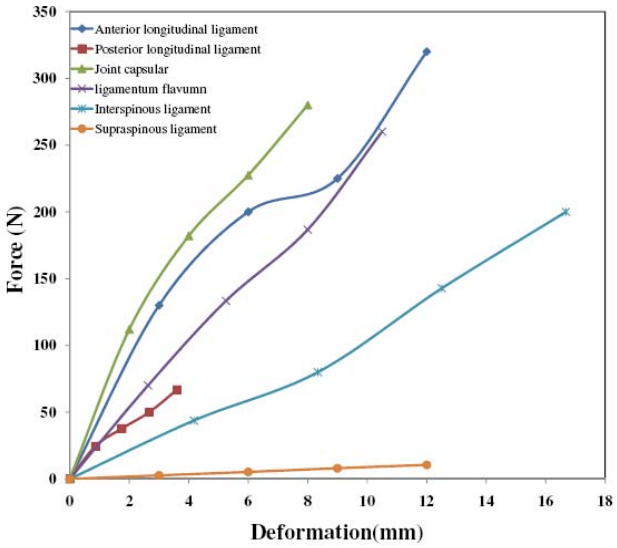

Fig 2. Force-deformation considered for ligaments [8].

Table 2 Physiological cross-sectional areas (PCSA) for muscles on each side of the spine given for individual fascicles identified by their insertion levels (mm^2)

Muscles	Lumbar Vertebra				
	L1	L2	L3	L4	L5
IP	252	295	334	311	182
MF	96	138	211	186	90
QL	88	80	75	70	-
LG	79	91	103	110	116
IC	108	154	182	189	-

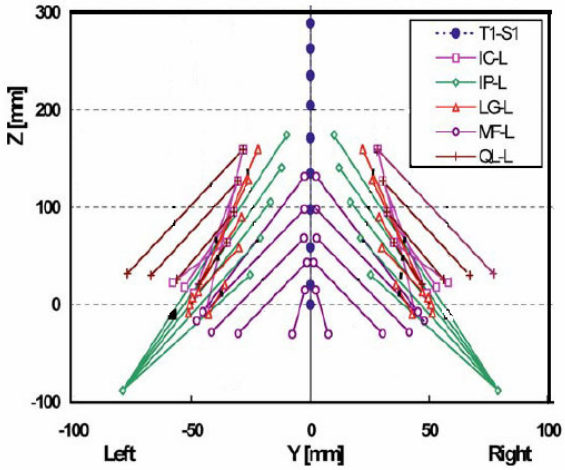

Fig 3. Representation of local musculature in the coronal plane used in the L_1-L_5 model

proximal femur). The architecture and physiological cross-sectional areas (Table 2) are taken based on published works [14, 16, 17, 24, 25].

A novel algorithm-a kinematics-based muscle force evaluation, coupled with optimization-is employed to solve for the redundant active–passive system subjected to prescribed kinematics (previously evaluated optimal postures) and applied external loads. In general, under given gravity + external loads, the rotations and translations at various levels (as many displacements at as many levels as are available) are prescribed. Subsequently, the required moments and forces (corresponding to prescribed displacements) are evaluated by the nonlinear finite element model. These moments and forces are subsequently fed into a separate algorithm that partitions them among muscles at each level, based on the equilibrium considerations and

instantaneous configuration of muscles. The axial compression penalties of these muscle forces (i.e., the axial component of muscle forces that may not yet have been considered) are then fed back into the finite element model as additional, updated external compression loads. This iterative approach is continued at each load step until convergence is reached (i.e., the magnitude of muscle forces in two consecutive iterations remains almost the same) If the horizontal translational (and/or rotational) degrees of freedom are not prescribed, the shear loads (and/or moments) of the muscle forces should also be applied in their respective directions, along with the compression penalties. In this manner, calculated muscle forces at each instance of loading are compatible with the prescribed kinematics (i.e., posture) and external/internal loading, while accounting for the nonlinear stiffness of the passive

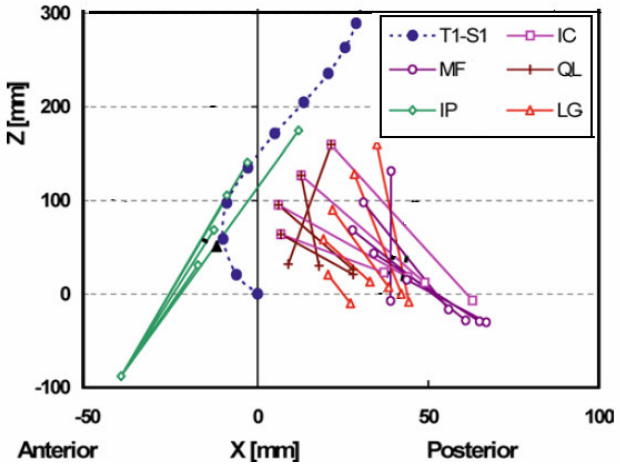

Fig 4. Representation of local musculature in the sagittal plane used in the L_1-L_5 model (IC iliocostalis, IP iliopsoas, LG longissimus, MF multifidus, QL quadratus lumborum,

system. As can be seen, such an approach exploits kinematics data to generate additional equations at each lumbar level, in order to alleviate the kinetic redundancy of the problem. If an insufficient number of prescribed displacements are available at a level to solve for unknown muscle forces at the same level, then an optimization approach should also be used. In the current study, since only sagittal rotations are prescribed, an optimization approach is needed.

The criterion used for optimization was the minimization of the sum of the cubed stresses in all lumbar levels. Thus the following cost function was employed:

$$Cost = \sum_{j=1}^{m} \left(\frac{F_j}{pcsa_j}\right)^3 \quad (1)$$

where Fj and $pcsa_j$ are the force magnitude and the physiological cross-sectional area of the jth muscle slip, respectively, and m is the number of muscle slips at each level.

The imposed constraints (Eq. (2)) are: the moment equilibrium, the fact that muscle forces must be equal to or greater than zero, and the muscle stresses must not exceed the maximum permissible stress.

$$\sum_i (r_i \times F_i u_i) - M = 0$$

$$\frac{F_i}{pcsa_i} \leq S \quad (2)$$

$$F_i \geq 0$$

where r_i and u_i are, respectively, the vector from the each segment disc center to the centroid of muscle slip 'i' and the unit vector representing the direction of muscle slip 'i'; the symbol '×' is the vector cross product; M is the reactive moment (net reaction) at the each level, and S is the maximum permissible muscle stress that is 0.5MPa [21]. Optimization algorithm performed using the Matlab optimization toolbox.

3. Results

3.1 Model validation

The kinematics data of the lumbar spine in Yamamoto et al.'s study [18] and Chen-Sheng Chen et al.'s studies [19] were compared to our results of the FEM under the act of the same load as listed in Table 3, 4, 5.

3.2 Described posture

The detailed L1-L5 model exhibits hypermobility (i.e. instability) under compression loads as low as 100 N when left unconstrained and fixed only at the base. To examine the lumbar response under meaningful compression loads of up to 2800 N, the segmental sagittal/lateral rotations at the L1 L5 levels are constrained, thus requiring relatively large equilibrating moments reaching ~22 N-m Under a total of 2800 N axial compression, the application of flattening of the lumbar spine substantially decreases the equilibrating moments at the L2-L5, levels thus requiring much less local muscle activation at these levels. A case example, arrived at by trial and error, with nearly minimum

Table 3 Comparison between the FEM results and the in vitro experimental study [18] and FEM Studies [19] in the three-dimensional angular motion of the L1–L5 lumbar spine under 10N.m flexion moment.

	Present Study	Yamamoto et al. (1989)	Chen-Shen Cheng et al (2001)
L_1-L_2(degree)	3.2	4.2	3.05
L_2-L_3(degree)	3	5.4	3.28
L_3-L_4(degree)	3.4	6.1	3.58
L_4-L_5(degree)	4.06	7.1	4.49

Table 4. Comparison between the FEM results and the in vitro experimental study [18] and FEM Studies [19] in the three-dimensional angular motion of the L1–L5 lumbar spine under 10N.m extension moment.

	Present Study	Yamamoto et al. (1989)	Chen-Shen Cheng et al (2001)
L_1-L_2(degree)	3	2.8	2.64
L_2-L_3(degree)	3.3	3.3	2.32
L_3-L_4(degree)	3.91	2.3	1.18
L_4-L_5(degree)	3.68	4	3.98

Table 5. Comparison between the FEM results and the in vitro experimental study [18] and FEM Studies [19] in the three-dimensional angular motion of the L1–L5 lumbar spine under 10N.m Lateral bending moment

	Present Study	Yamamoto et al. (1989)	Chen-Shen Cheng et al (2001)
L_1-L_2(degree)	2.75	3.3	2.85
L_2-L_3(degree)	3.36	5.0	3.31
L_3-L_4(degree)	3.68	4.3	3.33
L_4-L_5(degree)	2.13	3.8	2.08

Table 6. Predicted muscle forces on each side for the cost function of minimum sum of cubic power of muscle stresses at each level under optimal posture and 2800 N compression

Level Vertebra	Muscle force (N)				
	IC	IP	LG	MF	QL
L1	0.21	1.34	0.12	0.32	0.23
L2	0.22	0.53	0.12	0.24	0.11
L3	2.74	5.83	1.13	6.15	1.15
L4	0	2.14	.02	0	0
L5	-	0	2.8	6.31	-

moments involves 12.64° at L1, 7.95° at L2, 4.45° at L3, -2.02° at L4 and -1.54° at L5.

3.3 Muscle forces

Small muscle forces are calculated for the foregoing optimal posture, as given in Table 6 at various lumbar levels for cost functions of cubic muscle stress. The cost function of the sum of cubic power of muscle stresses activates more muscles than the other cost functions.

4. discussion

The redundancy in the trunk active system can serve to balance the varying external moments along the spine, actively augmenting the stiffness of the system by adequate activation level, and controlling posture in order to minimize active muscle forces and passive tissue stresses and strains. A number of methods have been proposed to solve for the highly redundant problem of spinal active-passive postural control and load distribution (e.g. Gagnon and co-workers [21]). Due to the shortcomings in existing reduction, optimization and EMG-driven models, and combinations thereof, a novel kinematics-based approach is proposed that thoroughly utilizes the passive-active synergy. In this method, the available, often measured, data on kinematics of the spinal column while performing a task is exploited to generate additional equations to solve for unknown muscle forces at different levels. Unlike the previous methods, therefore, the computed solution satisfies

simultaneously the kinematics and kinetics requirements at all levels along the entire length of the spine during a particular activity. It also allows for the subsequent verification of the stability of the posture at any given load, though not performed in this work.

References:

[1] A. Shirazi-Adl S. Sadouk M. Parnianpour D. Pop M. El-Rich., 2002. Muscle force evaluation and the role of posture in human lumbar spine under compression. Eur Spine J (2002)

[2] Antonius Rohlmann, Lars Bauer, Thomas Zander, Georg Bergmann, Hans-Joachim Wilke., 2006. Determination of trunk muscle forces for flexion and extension by using a validated finite element model of the lumbar spine and measured in vivo data. Journal of Biomechanics 39 (2006) 981–989

[3] De Luca, C.J., 1997. The use of surface electromyography in biomechanics. Journal of Applied Biomechanics

[4] Francisco Ezquerro □, Antonio Simo´n, Marı´a Prado, Ana Pe´rez. Combination of finite element modeling and optimization for the study of lumbar spine biomechanics considering the 3D thorax– pelvis orientation. Medical Engineering & Physics 26 (2004).

[5] Yabo Guan Æ Narayan Yoganandan Æ Jiangyue Zhang Æ Frank A. Pintar Æ Joesph F. Cusick Æ Christopher E. Wolfla Æ Dennis J. Maiman Validation of a clinical finite element model of the human lumbosacral spine. Med Bio Eng Comput (2006)

[6] Chen-Sheng Chen, Cheng-Kung Cheng, Chien-Lin Liu, Wai-Hee Lo Stress analysis of the disc adjacent to interbody fusion in lumbar spine. Medical Engineering & Physics 23 (2001)

[7] Gagnon D, Larivière C, Loisel P (2001) Comparative ability of EMG, optimisation, and hybrid modelling approaches to predict trunk muscle forces and lumbar spine loading during dynamic sagittal plane lifting. Clin Biomech

[8] Frank A. Pintar, Narayan Yoganandan, Thomas Myers, Ali Elhagediab, Anthony Sances JR. (1992). Biomechanical properties of human lumbar spine ligaments. J.Biomechanics

[9] Zheng-Cheng Zhonga, Shun-Hwa Wei a, Jung-Pin Wang b, Chi-Kuang Feng c, Chen-Sheng Chena, Chung-huang Yu a Finite element analysis of the lumbar spine with a new cage using a topology optimization method. Medical Engineering & Physics 28 (2006)

[10] Kiefer A, Shirazi-Adl A, Parnianpour M (1997) On the stability of human spine in neutral postures. Eur Spine J 6:45–53

[11] Kiefer A, Shirazi-Adl A, Parnianpour M (1998) Synergy of human spine in neutral postures. Eur Spine J 7:471– 479

[12] McGill, S.M., 1992. A myoelectrically based dynamic three-dimensional model to predict loads on lumbar spine tissues during lateral bending. Journal of Biomechanics 25, 395}414

[13] Shirazi-Adl A, Parnianpour M (1999) Effect of changes in lordosis on mechanics of the lumbar spine lumbar curvature in lifting. J Spinal Disord 12:436–447

[14] Dumas GA, Poulin MJ, Roy B, Gagnon M, Jovanovic M (1991) Orientation and moment arms of some trunk muscles. Spine 16:293–303

[15] Panagiotacopulos ND, Pope MH, Krag MH, Block R. Water content in human intervertebral discs. Part I. Measurements by magnetic resonance imaging. Spine 1987;12:912–7.

[16] Bogduk N, Macintosh JE, Pearcy MJ (1992) A universal model of the lumbar back muscles in the upright position. Spine 17:897–913

[17] Han JS, Ahn JY, Goel VK, Takeuchi R, McGowanD(1997) CT-based geometric data of human spine musculature, Part 1. Japanese patients with chronic low back pain. J Spinal Disord 5:448–458

[18] Yamamoto I, Panjabi MM, Crisco T, Oxland T. Three-dimensional movement of the whole lumbar spine and lumbosacral joint. Spine 1989

[19] Chen-Sheng Chen a, Cheng-Kung Cheng a,*, Chien-Lin Liu b, Wai-Hee Lo. Stress analysis of the disc adjacent to interbody fusion in lumbar spine. Medical Engineering & Physics 23 (2001)

[20] Wilke, H.J., Claes, L., Schmitt, H., Wolf, S., 1994. A universal spine tester for in vitro experiments with muscle force simulation. European Spine Journal 3, 91–97.

[21] Gagnon D, Larivie`re C, Loisel P (2001) Comparative ability of EMG, optimisation, and hybrid modelling approaches to predict trunk muscle forces and lumbar spine loading during dynamic sagittal plane lifting. Clin Biomech (Bristol, Avon) 16:359–372